

Trait–demography relationships underlying small mammal population fluctuations

Koen J. van Benthem^{*1}, Hannah Froy^{*2}, Tim Coulson ³, Lowell L. Getz ⁴, Madan K. Oli ⁵, Arpat Ozgul ¹

¹ Department of Evolutionary Biology and Environmental Studies, University of Zurich

² Institute of Evolutionary Biology, University of Edinburgh

³ Department of Zoology, University of Oxford

⁴ Department of Animal Biology, University of Illinois

⁵ Department of Wildlife Ecology, University of Florida

* These authors contributed equally to this work

Corresponding author: Koen van Benthem, koen.vanbenthem@ieu.uzh.ch

Keywords

body mass, integral projection models, phenotypic plasticity, population ecology, population regulation, small mammal population fluctuations, trait–based demography, trait dynamics.

Summary

1. Large-scale fluctuations in abundance are a common feature of small mammal populations and have been the subject of extensive research. These demographic fluctuations are often associated with concurrent changes in the average body mass of individuals, sometimes referred to as the “Chitty effect”. Despite the long-standing recognition of this phenomenon, an empirical investigation of the underlying coupled dynamics of body mass and population growth has been lacking.
2. Using long-term life-history data combined with a trait-based demographic approach, we examined the relationship between body mass and demography in a small mammal population that exhibits non-cyclic, large-scale fluctuations in abundance. We used data from the male segment of a 25-year study of the monogamous prairie vole, *Microtus ochrogaster*, in Illinois, USA. Specifically, we investigated how trait–demography relationships and trait distributions changed between different phases of population fluctuations, and the consequences of these changes for both trait and population dynamics.
3. We observed phase-specific changes in male adult body mass distribution in this population of prairie voles. Our analyses revealed that these changes were driven by variation in ontogenetic growth, rather than selection acting on the trait. The resulting changes in body mass influenced most life-history processes, and these effects varied among phases of population fluctuation. However, these changes did not propagate to affect the population growth rate due to the small effect of body mass on vital rates, compared to the overall differences in vital rates between phases. The increase phase of the fluctuations was initiated by enhanced survival, particularly of juveniles, and fecundity whereas the decline phase was driven by an overall reduction in fecundity, survival and maturation rates.
4. Our study provides empirical support, as well as a potential mechanism, underlying the observed trait changes accompanying population fluctuations. Body size dynamics and population fluctuations resulted from different life-history processes. Therefore, we conclude that body size dynamics in our population do not drive the observed population dynamics. This more in-depth understanding of different components of small mammal population fluctuations will help us to better identify the mechanistic drivers of this interesting phenomenon.

Introduction

The ubiquity of large-scale fluctuations in population size exhibited by small mammals living at high latitudes is one of the oldest enigmas in population biology (Elton 1924). Periodic fluctuations in abundance have been documented in small mammal species with a wide variety of life-history strategies and in a range of different habitats (Krebs & Myers 1974). Various explanations for the existence of such fluctuations have been proposed, such as resource limitation (Turchin & Batzli 2001), predation (Hanski, Hansson & Henttonen 1991), stress response (Christian 1950, Christian & Davis 1966), or interactions between these factors (Lidicker 1988, Lidicker & Ostfeld 1991, Andreassen et al. 2013). It has also been suggested that the occurrence of periodic fluctuations is due to a combination of extrinsic and intrinsic factors, although evidence remains scarce (Stenseth, Bjornstad & Falck 1996, Andreassen et al. 2013, but see Radchuk, Ims & Andreassen 2016). Importantly, a consensus on how these processes affect both the amplitude and periodicity of the fluctuations has not yet been reached (Batzli 1996, Krebs 1996, Krebs 2013).

Although the ultimate drivers of population fluctuations may be unknown, we do know that they are underlain by demographic processes (Elton 1924). Population growth rate is directly influenced by survival and reproduction, whereas other life-history parameters such as growth, offspring body size, and maturation influence population size indirectly (De Kroon, Van Groenendael & Ehrlén 2000). Linking population fluctuations with the underlying demographic processes is essential if we are to develop a better understanding of population fluctuations (Stenseth 1999, Lima et al. 2001, Ozgul, Getz & Oli 2004). Furthermore, an increasing number of long-term individual-based studies are reporting feedback mechanisms between phenotypic traits and demography in changing environments (e.g. Coulson et al. 2011). Fitness-related individual traits such as body mass can vary over ecological timescales due to variation in density-dependent and -independent processes (Ozgul et al. 2014). Resulting changes in trait distributions or in trait–demography relationships can alter demographic rates, which in turn can influence individual fitness (Pelletier et al. 2007) as well as population dynamics (Ozgul et al. 2010). Trait–demography relationships are relevant in the context of small mammal population fluctuations since many of these populations exhibit phase-related changes in mean body mass, a phenomenon first described by Chitty (1952).

Integral projection models (IPMs) are increasingly used to examine the relationship between phenotypic traits and demography (Easterling, Ellner & Dixon 2000, Ellner & Rees 2006, Coulson et al. 2011, Coulson 2012, Merow et al. 2014). Whereas matrix population models (Caswell 2001) assume homogeneity of survival and reproduction within each life-history stage, IPMs allow these processes to be characterised also by a continuous phenotypic trait, which allows heterogeneity within a life-history stage (Ellner & Rees 2006). Using a matrix approximation of the IPM, one can follow the distribution of trait values and the population size through time, and quantify how they are affected by changing phenotype–demography relationships. This approach means we can utilise methods that have been developed for matrix models to study the joint dynamics of different demographic and trait-transition processes that are linked through the life cycle. To investigate the effect of trait dynamics on population dynamics, for example, it is important to look at, not only the ontogenetic growth, but also the changing age structure, selection, and inheritance. An IPM allows this by linking these processes.

In this study, we used the male segment of a 25-year dataset from an individually marked population of prairie voles, *Microtus ochrogaster*, to investigate the links between a phenotypic trait (male body mass) and population dynamics in a small mammal population which exhibits large-scale, but non-cyclic fluctuations in abundance. We used a phenomenological approach to investigate how the relationships between body mass and demographic rates differed among different phases of the population fluctuations. We then used these relationships to construct an integral projection model. Using this model, we identified the key life-history processes underlying the phase-related changes in both population growth rate and in body mass distributions. Although our methodology does not allow for the identification of the ultimate population-extrinsic or -intrinsic drivers underlying the population fluctuations, our results do provide further insight into the concurrent dynamics of body mass and population growth in small mammal fluctuations.

Methods

Study System and Data Collection

Our data come from a 25-year mark–recapture study of a prairie vole population in an alfalfa (*Medicago sativa*) field in the University of Illinois biological research area, Illinois (40°15'N, 88°28'W) (Getz et al. 2006). The prairie vole inhabits prairie and agricultural habitats throughout the prairie states of North America (Linzey & Hammerson 2008). They

reproduce throughout the year, with a peak between May and October (Stalling, 1990). Average litter size in field populations is 3.5 pups, and males can sire a litter from the age of 49 days onwards (Stalling 1990). Population size fluctuates substantially; previous work has shown that population fluctuations are primarily driven by births and deaths, rather than immigration and emigration of individuals (Getz et al. 2006). Monthly trapping sessions took place between May 1972 and 1997, with the ID, sex, body mass (to the nearest 1g), and reproductive condition of individuals recorded at each capture (Fig. 1). Trapping occurred in either of two adjacent 1ha subfields. Over the course of the study, the trapping grid was moved four times between these subfields to ensure adequate habitat (alfalfa). Voles from the old subfield would colonize the new subfield and population density was essentially the same before and after moving the trapping grid. We therefore consider all trapping data to be stemming from one single population. Further details on the field procedures can be found in Getz et al. (2005).

Data Analysis

We used data collected from only the male segment of the population in our analyses, due to the confounding effect of pregnancy on female body mass. Given the strongly monogamous mating system and unbiased primary sex ratio, analysis of the male segment of the population most likely reflects overall population dynamics (Getz et al. 2005). This is well supported by the similarity in number of captured individuals and average adult body mass between males and females (Supplementary Information S1). In total, there were 6484 observations of 3765 males. Males were grouped into two stages based on reproductive status: juveniles were characterised as individuals that were not yet reproductively active (testes still abdominal), and adults as individuals that were either reproductive (scrotal testes) in the current month or in any previous month. All analyses were performed in the statistical programming package R (v. 3.1.0, 2015).

Body mass, demography and trait-transition rates

We first examined the relationships between body mass and the various monthly demographic rates, which account for changes in the number of individuals in the population. Our response variables were: juvenile and adult survival probability (S_j and S_a : the stage-specific probability of a male surviving from month t to month $t+1$); maturation probability (M : the probability of a juvenile in month t transitioning to an adult in month $t+1$, conditional on survival); reproduction probability (R : the probability of an adult being reproductively

active in month t); and per capita fecundity (F : the number of male juveniles produced in month $t+1$ per reproductively active male in month t). We also modelled the relationship between male body mass and the monthly trait-transition rates, which account for transitions in individual trait values. The trait-transition rates were: ontogenetic growth (G : change in body mass of a male from month t to month $t+1$); and inheritance of offspring mass (D : body mass of recruits in month $t+1$ as a function of paternal mass in month t). In all models we tested for the effect of population density phase in addition to the effect of body mass. We did this by assigning each month to one of the four phases of a population fluctuation: increase, peak, decline or trough (Fig. 1a; Getz et al. 2001) and including phase as a fixed categorical variable in our models. The assignment of the phases to each month was performed in a reproducible and objective way, using a peak deconvolution algorithm using the R package “peaks” (Morhac 2012) on the number of captured individuals. The results of this assignment were in close agreement with previously used manual approaches (Ozgul, Getz & Oli 2004, Goswami et al. 2011).

Individual-level data were available for survival, maturation, reproduction and growth. Survival and maturation rates were estimated using a multistate mark–recapture model implemented using Program MARK (White & Burnham 1999) with the RMark interface (Laake & Rexstad 2010). Reproduction and growth rates were modelled using generalised additive models (GAMs; Wood 2006) including random effects for repeated measures of individuals and months. Growth was modelled using Gaussian error distribution, and reproduction probability using a binomial error distribution and logit link function. Non-linear effects of body mass on the demographic rates were tested using quadratic effects in the mark–recapture analysis (survival and maturation probability), and splines in GAMs (reproduction probability and growth).

Individual-level data were not available for per-capita fecundity and offspring mass, so these variables were estimated using population-level data. Furthermore, we did not detect a mass effect in fecundity and included only the phase effect. Very few offspring are captured in traps before they emerge from their nests at 15–20 days old. Counts of very small individuals are, therefore, negatively biased. In addition, it is difficult to determine whether larger juveniles were the products of matings during the previous month (and therefore new recruits), or whether they were already born the previous month. We overcome these difficulties by focusing on the number of captured individuals in month t with a body mass between 15 and 25g ($N_{j*}(t)$). Because juveniles are estimated to gain 1g/day over the first

month of life (Stalling 1990), individuals within this 10g range were assumed to be the products of matings that occurred over a 10-day period in the previous month. We multiply $N_{j*}(t)$ by three (30 days / 10 days) and divide by the corresponding juvenile recapture rate $P_j(t)$ to estimate the number of recruits in month t . The number of parents was estimated as the number of captured reproductive individuals divided by the appropriate recapture rate, $N_r(t)/P_a(t)$. To obtain the per-capita fecundity for a given phase, $F(phase)$, we divided the total number of recruits from this phase by the total number of parents in this phase. The sums are taken over all time steps that are in each phase:

$$F(phase) = 3 \cdot \frac{\sum_{t \in phase} \frac{N_{j*}(t+1)}{P_j(t+1)}}{\sum_{t \in phase} \frac{N_r(t)}{P_a(t)}}$$

Offspring mass was estimated as the mean body mass of the recruits. These population-level estimates were modelled as a function of average body mass, with non-linear effects tested using GAM splines. Offspring mass was modelled using a Gaussian error distribution.

To test for variable effects of body mass during different phases of the population fluctuations, we included a two-way interaction between body mass and phase in all models that used individual-level data (data were insufficient for variables estimated at the population level). Model selection was performed using Akaike Information Criterion corrected for small sample size (AICc) where the best model is taken to be that with the lowest AICc value (Burnham & Anderson 2002). Furthermore we added season as a fixed covariate to the selected models to evaluate to what extent phase-specific effects could be explained by seasonality (see Supplementary Information S2 for more details). Finally, to test the hypothesis that maturation rates decrease as the increase phase gets closer to the decline, we also tested for the effect of increased population density on maturation rates during the increase phase, by including the minimum number of individuals alive as a time-varying covariate of the maturation rate.

Modelling population and trait dynamics

We used a stage- and trait-structured integral projection model (IPM, equations shown below) to understand how the trait-demography relationships influenced the overall population and trait dynamics in each phase (p).

$$n_a(z, t + 1) = \int_{z'} S_j(z' | p) M(z' | p) G(z | z', p) n_j(z', t) dz' + \int_{z'} S_a(z' | p) G(z | z', p) n_a(z', t) dz'$$

$$n_j(z, t + 1) = \int_{z'} S_j(z' | p) (1 - M(z' | p)) G(z | z', p) n_j(z', t) dz' \\ + \int_{z'} R(z' | p) F(z' | p) D(z | z', p) n_a(z', t) dz'$$

We assumed a life cycle with two life-history stages (with a trait distribution for juveniles, n_j and adults, n_a), and focused on body mass (z) as the main trait at time t . We constructed an IPM for each of the four phases of a population fluctuation, based on the phase dependency in the underlying functions (S_j , S_a , M , G , R , F , D). The most parsimonious model structure for each demographic and trait-transition rate identified above were used to parameterise the phase-specific IPMs. Average reproduction probability was calculated using sampling. The rationale for doing so and an explanation of the process is further described in the Supplementary Information S3.

A retrospective perturbation analysis was then performed to evaluate how differences in demographic and trait-transition functions between phases propagate to differences in asymptotic population growth rates between phases (e.g., Ozgul et al. 2010, Bruna et al. 2014). This analysis is conceptually equivalent to the fixed LTRE analysis as described by Caswell (2001). Phases were compared pairwise. For each pair, composite IPMs were constructed from the seven functions describing the demographic and trait-transition rates, where each function could vary independently between the two phases. In total, 128 IPMs with all possible combinations of seven functions from the two phases were constructed, and for each of these IPMs, the asymptotic population growth rate (λ) was calculated as the dominant eigenvalue (for a schematic depiction, see Fig. 2; a mathematical treatment of this analysis is given in Supplementary Information S4). The variation in λ values among these 128 IPMs are caused by differences in the underlying functions between the two phases. Next, a linear model was used to assess the amount of variation in λ explained by the phases for which each of the seven functions was parameterized. This resulted in a 128x8 design matrix, in which the columns correspond to the seven functions and an intercept, and the rows to the different composite IPMs. This matrix consisted of binary coding indicating the phase for which each function was parameterized. The column for the intercept contained only ones. A linear model was then run for each phase transition, with λ as the response variable and the design matrix binary data as explanatory variables. This allowed us to

examine the effect of changes in each of the seven functions on the asymptotic growth rate, and thereby identify the key life history processes responsible for the shift in growth rate between phases.

We performed this perturbation analysis for three phase transitions: trough to increase; increase to decline and decline to trough. The peak phase was not included in this analysis because the peak phases were very brief and lacked detailed data. However, they helped to demarcate increase and decline phases and provided information on the vital rates, and so we retained all four phases in our models of demography and trait-transition rates. We then repeated this analysis with the models that also contained seasonality to test whether seasonality can account for the phase-specific patterns.

Because the analysis of the asymptotic population growth rate ignored the transient effects of stage- and mass-structure, we repeated the non-seasonal perturbation analysis using the transient population growth rate instead of λ as a response variable. This allowed us to check if the asymptotic results are representative for more realistic time scales. For this analysis, we used the average population vector of the initial phase, projected this vector iteratively over four months, and then took the geometric mean of the four monthly growth rates to be the transient population growth rate. We then investigated the effect of changing each of the seven demographic and trait-transition functions (as above). To investigate immediate transient effects, the transient analyses were also performed over a single time step (Supplementary Information S5).

Finally, we repeated the same asymptotic and transient retrospective perturbation analyses to investigate the phase-related changes in adult body mass dynamics. For the asymptotic analysis, this involved examining changes in the mean adult body mass of the stable mass distribution, whereas for the transient analysis, this was the mean adult body mass of the population vector projected over four months. This approach was pursued to enable us to track the joint effect of the seven underlying functions. Otherwise, it is not possible to determine the effect of, for example, maturation rate on average adult body mass without taking into account average juvenile body mass and juvenile survival. When comparing the perturbation analysis for the population growth rate and average adult body mass, it is important to note that these analyses are based on observed correlations and we can thus only make inferences on the coupling between trait and population dynamics, not on their mutual causality.

Results

Life-history processes

Male adult body mass varied among phases of the population fluctuations, with higher masses recorded during the increase and peak phases (mean \pm se: $39.59 \pm 0.15\text{g}$), and lower masses during the decline ($38.39 \pm 0.17\text{g}$) and trough ($36.34 \pm 0.35\text{g}$) phases (Fig. 1b).

Recapture rates were generally higher for adults, ranging from 0.51 ± 0.04 in the trough phase to 0.69 ± 0.03 in the peak phase, than juveniles, ranging from 0.11 ± 0.03 during increase to 0.34 ± 0.04 during decline (Table 1). Adult survival varied among phases, being highest during the increase (0.72 ± 0.06) and lowest during the decline phase (0.34 ± 0.04 , all rates are monthly and estimated for the average body mass for the corresponding phase).

The relationship between male body mass and survival varied among phases as indicated by the support for the interaction term between body mass and phase in the final model (Table 1). The optimal body mass at which adult survival was the highest shifted to lower values during the decline phase (Fig. 3b). The juvenile survival–body mass relationship generally showed an increase in survival with body mass that levelled off at higher juvenile body masses. The slope of this relationship (i.e., the survival selection differential) was the weakest during the decline phase (Table 1, Fig. 3a). The described patterns did not change when we added season (Supplementary Information S2, Fig. S2.2).

Maturation rate varied among phases, being highest during the increase (0.53 ± 0.05) and lowest in the decline phase (0.21 ± 0.03 ; Fig. 3c). During the increase phase, maturation rate was negatively correlated with population density (-0.02 ± 0.006), indicating that males were less likely to mature closer to peak densities. Furthermore, maturation was influenced by season, with higher maturation rates in spring and summer (Supplementary Information S2, Fig. S2.2). Importantly, however, the difference in maturation rate between phases depended only weakly on the season.

Reproduction probability was generally very high (Fig. 3d) especially during increase (0.96 , 95% CI: 0.92 - 0.98) and peak (0.93 , 95% CI: 0.80 - 0.99) and slightly less so during trough (0.87 , 95% CI: 0.79 - 0.93) and decline (0.84 , 95% CI: 0.73 - 0.91). Reproduction probability was positively correlated with male body mass, and this was more evident during the decline phase (Fig. 3d). This effect was due to the implicit interaction between phase and mass caused by the logit transformation; no interaction was found on the scale of the linear

predictor (Table 1, also see Ai & Norton 2003). When accounting for seasonality, the reproduction probability was no longer lower in the decline phase than in the trough and increase phase (Supplementary Information S2, Fig. S2.2). The low reproduction probability observed during decline was due to the decline phase mainly occurring in winter, and reproduction probability being low in winter. The low reproduction probability in the decline phase is thus actually a seasonal effect and not a phase specific effect.

Per capita fecundity varied solely among phases, being highest during the increase (3.25, 95% CI: 2.74-3.88) and trough phase (1.97, 95% CI: 1.45-2.61) and lowest in the decline (0.67, 95% CI: 0.51-0.87) and peak phase (1.05, 95% CI: 0.74-1.38). Here confidence intervals are based on 10,000 bootstrapping samples independently drawn for each phase.

We initially tested for stage-specific individual growth rates, but including stage in the model as a fixed effect did not improve model fit ($\Delta\text{AICc} = +1.93$, Table 1), so we continued with a single growth function. Growth was slower during the decline phase (0.96 ± 0.34 g/month for average-sized individual) than the increase (3.43 ± 0.30), peak (3.47 ± 0.62) and trough (2.78 ± 0.40) phases. The relationship between body masses at time t and $t+1$ was non-linear (Table 1, Fig. 3e) and the relationship did not change when accounting for seasonality (Supplementary Information S2, Fig. S2.2). This relationship varied between phases as indicated by the statistically supported interaction term. Males with lower body mass grew at a faster rate than heavier males. The heaviest males tended to lose weight; this effect was particularly apparent during the decline phase (Fig. 3e). However, this regression to the mean may be partially caused by fluctuations around the actual body mass value.

There was no evidence that mean paternal body mass influenced offspring body mass. However, offspring mass varied among phases, with mass being slightly higher during the decline (21.83 ± 0.29 g) compared to the other phases (ranging from 19.80 ± 0.63 g to 20.46 ± 0.27 g) (Table 1).

Population and trait dynamics

When the most parsimonious models for each life-history process were used to parameterise phase-specific IPMs, the resulting asymptotic population growth rates (λ) naturally varied among phases: increase=1.54; peak=1.12; decline=0.69; trough=0.96. This variation in λ among phases was much larger than the variation among seasons (Supplementary Information S2, Fig. S2.3). The retrospective perturbation analysis highlighted the changes in

333 trait–demography relationships that contributed the most to the changes in λ and in mean
334 adult body mass between consecutive phases.

335 The perturbation analyses explained most of the variation in estimated population growth rate
336 and average male adult body mass ($R^2 > 0.95$ for all linear models of the perturbation
337 analyses). Changes in life-history processes differentially affected the phase transitions (Fig.
338 4). In particular, the increase in juvenile survival and fecundity was the main trigger for the
339 initiation of the increase phase (Fig. 4a). Subsequently a decrease in fecundity followed by
340 those in survival and maturation, were responsible for the substantial drop in λ from increase
341 to decline phase (Fig. 4b). Finally, the halting of the population decline (i.e., transition into
342 trough phase) was caused mainly by an increase in fecundity, followed by increases in
343 maturation and adult survival (Fig. 4c). Although there was some variation in reproduction
344 probability, growth and offspring mass, these variables had little impact on the population
345 dynamics (Fig. 4a-c). For example, growth varied among phases (Fig. 3e), but this variation
346 did not have a major influence on phase transitions (Fig. 4a-c). We repeated the perturbation
347 analysis with an interaction between juvenile survival and fecundity and an interaction
348 between adult survival and fecundity in the final model, but this did not alter the outcomes
349 (results not shown). Seasonality did also not alter the outcomes (Supplementary Information
350 S2, Fig. S2.4).

351 The main driver of the change in the mean male adult body mass among phases was the
352 changing ontogenetic growth of individuals (Fig. 4d-f). Males grew faster during the increase
353 phase leading to larger masses, and this pattern reversed during the decline phase, decreasing
354 their average body mass. Maturation and fecundity showed counteracting influence on the
355 changing male adult mass; however, compared to growth, these effects were small. In the
356 body mass analysis, again, adding season did not alter these results (Supplementary
357 Information Fig. S2.5).

358 The results of the transient perturbation analysis were very similar to the asymptotic analysis
359 for both population growth rate and average male adult mass (Fig. 4), indicating that the
360 observed average distributions matched well with the stable stage and mass distributions
361 within each phase.

362 Discussion

Our analysis, based on one of the longest running small mammal population studies, provides empirical support for changes in male body mass distributions accompanying large-scale fluctuations in population size, and proposes a mechanism underlying these observed changes in trait dynamics. The changes in body mass distributions were caused by phase-specific changes in ontogenetic growth and not by selection acting on the trait. The resulting changes in body mass affected most vital rates and trait-transition functions, and these effects varied among the phases of the population fluctuations. Overall, the phase-specific effects on survival and reproduction were stronger than the effects due to the variation in average male body mass, thereby limiting the extent to which variation in body mass propagated to the population dynamics. Fig. 4d-f highlights that phase specific changes in ontogenetic growth had a strong influence on average male adult body mass, this variation did, however, not lead to changes in population growth rate (Fig. 4a-c). The demographic causes of the observed population fluctuations were therefore generally trait-independent effects. The increase phase was initiated by enhanced juvenile survival and fecundity, whereas the decline phase was driven by an overall collapse primarily in fecundity, followed by collapses in juvenile survival and maturation. This suggests that the observed fluctuations in abundance in our population are mainly driven by trait-independent changes in the recruitment components of the life cycle.

The population fluctuations were accompanied by variation in average male adult body mass, which was higher during the increase and peak phases, as observed in many other small mammal populations (Lidicker & Ostfeld 1991, Krebs 1996). The difference in average male mass between increase and peak phases and the trough phase (~9%) is comparable to what was found in a study on *Microtus agrestis* (Burthe et al. 2010). This difference is however small in comparison to more frequently reported values 20-30% in studies that have documented a Chitty effect (as discussed in Burthe et al. 2010). When we investigated the underlying trait–demography relationships and how these changed between phases, we found that optimal body mass for male adult survival was highest during the increase phase and shifted to smaller males during the peak and decline phases. This selective disadvantage of large body mass at highest densities could be caused by predation of larger males if smaller males are more likely to use refuges and escape from predators (Sundell & Norrdahl 2002). Alternatively, it is possible that the advantages of being large are outweighed by the energetic costs of maintaining high body mass at high population densities. Competition can also increase at higher densities, and larger and superior (more aggressive) competitors for

territories and food resources can increase in number, leading to an increase in mean body mass, as previously reported for *Microtus ochrogaster* (Boonstra & Krebs 1979). However, although there is a clear change in survival selection on body mass, our perturbation analysis showed that this change played only a minor role in changing the average body mass. Instead, the somatic growth was the main driver behind body mass dynamics: individuals grew faster, longer, and consequently, to a larger body mass during the favourable conditions prior to peak densities, as also hypothesised by Lidicker & Ostfeld (1991). Indeed, our analysis shows that it was the higher somatic growth rather than the positive survival selection on body mass that caused the observed increase in average male adult mass during the increase phase. This is also in line with previous results on California voles, where prolonged periods during the increase phase favorable to growth and survival result in “giant individuals” (Lidicker & Ostfeld 1991). These “giant” male Californian voles had, however, no reproductive advantage and were even negatively associated with reproductively active females.

To properly disentangle plastic and evolutionary responses, however, it is necessary to estimate changes in the heritable part of the trait over time. Unfortunately we had no information on relatedness between individuals, and it was therefore not possible to estimate this. The closest proxy for genetic effects in our analysis was broad-sense inheritance, which included phenotypic plasticity, paternal effects, and heritability (Coulson et al, in review). We found little evidence for the importance of inheritance although our offspring body mass function was defined at the population level, and as such, was a proximate measure. For meadow voles (*Microtus pennsylvanicus*) an analysis of the heritability of body mass, as well as growth rate, and age and body mass at sexual maturity, was performed in a controlled population (Boonstra & Boag 1987). Heritability of all traits was found to be low in this species, which is consistent with our proximate findings in *M. ochrogaster*.

Our results showed that the increase phase was mainly initiated by a change in the juvenile survival function and fecundity. Although juvenile survival depended on body mass, from the shape of this function (Fig. 3a) it is apparent that juvenile survival was much more strongly influenced by the phase of the population fluctuation than by body mass (i.e. moving on the curves has a smaller effect than moving between curves in Fig. 3a). As a consequence, changes in average body mass do not propagate to influence the population growth rate substantially. Instead, population fluctuations are likely influenced by phase-specific extrinsic and intrinsic environmental effects, through a pathway that is body mass-independent. This interpretation is further supported by the fact that the most influential factor on changing

body mass (i.e. ontogenetic growth) has negligible influence on the population growth rate. Similarly, the demographic determinants of population collapse were mass-independent declines in fecundity, juvenile survival and maturation – which may be a direct effect of unfavourable environmental conditions on the recruitment component of the life cycle, consistent with theoretical expectations and empirical evidence on phase-related changes in maturation and juvenile survival in cyclic species (Oli & Dobson 1999, Oli & Dobson 2001, Ozgul, Getz & Oli 2004, Goswami et al. 2011). However, it has to be noted that fecundity may be partially confounded with immigration (it is not possible to definitively tell apart recruitment and immigration) and with reproductive probability (we cannot be certain that all males with scrotal testes have actually sired offspring). This also explains our relatively high reproduction probability and low fecundity. Further information on these potentially confounding factors might shift the contributions between reproductive probability and fecundity, but would not affect their cumulative effect.

Our approach is purely phenomenological and does not address the ultimate mechanisms underlying variation in the trait-demography relationships. Although the actual drivers of trait and population fluctuations remain to be explored, we tested for the potential confounding effects of seasonality. There is in fact some seasonality in the phases, with increase phases occurring more often in the summer and autumn, and decline phases occurring more often in the winter and spring. In a separate set of analyses (supplementary information S2), we added season as a covariate to all demographic and trait transition functions (except fecundity, due to data limitations). The reproduction probability and maturation rate showed the largest seasonal variation; however, the perturbation analysis including these seasonal effects (Fig. S2.4) showed a very similar pattern as the original analysis (Fig. 4).

In contrast to the asymptotic growth rates, the transient growth rates do not depend solely on the trait–demography relationships, but also on the standing population structure. However, the perturbation analysis on the transient growth rate over four months showed essentially the same pattern as the analysis of the asymptotic growth rate. Similarly, the transient analyses of the average adult body mass over four time steps showed strong similarities to the asymptotic analysis. These results indicate that the observed stage and mass distributions within each phase was rather stable, and the results of the asymptotic analysis gave an adequate representation of what happens on more relevant time scales.

Social and extrinsic environmental factors affect key life-history processes often through their influence on fitness-related phenotypic traits (Peters 1983, Calder 1984, Uchmanski 1985) and there is mounting evidence that variation in these traits can influence population dynamics (Grimm & Uchmański 2002, De Roos, Persson & McCauley 2003, Pelletier et al. 2007). Such variation is particularly pronounced in mammals living in socially structured populations and variable environments, where traits can vary within and among individuals as a consequence of adaptive adjustment to individual, social and environmental factors (e.g., O'Riain & Jarvis 1998, Buston 2003). Several studies on mammalian populations have recently demonstrated the role of trait dynamics in driving population dynamics (Ozgul et al. 2010, Ozgul et al. 2014), and in these studies, population dynamics were shown to depend more on the plastic changes in trait dynamics. Based on these observations, and the observation that body mass strongly influences fitness in many species (Kingsolver & Pfenning 2004) we expected body mass and population dynamics to be coupled. Considering the monogamous mating system and absence of sexual dimorphism, factors influencing body mass dynamics or coupling of body mass-population dynamics are unlikely to differ between males and females. Nonetheless, similar studies in female prairie voles would be needed to test this. If we assume that we are looking at the correct trait and the male segment adequately represents the trait and population dynamics, we can conclude that the observed changes in trait distributions are a phenotypic by-product rather than an integral driver of small mammal population fluctuations (also see Oli 1999, Norrdahl & Korpimäki 2002).

In conclusion, we have seen that population fluctuations in prairie voles are mainly caused by body mass-independent changes in the recruitment component of the life cycle. Male adult body mass itself did vary among phases, and the optimal body mass in terms of survival shifted among phases. This variation was, however, not the main driver of body mass fluctuations accompanying population fluctuations. Instead, trait dynamics were governed by ontogenetic growth, and to an extent, by counteracting effects of maturation and fecundity. This combination of results mainly points in the direction of plastic rather than selection processes governing the trait dynamics. Although we found evidence that body mass distribution influenced some demographic rates, our results suggest that the dynamics of this fluctuating population were primarily driven by trait-independent effects. We can conclude that if individual quality is driving the population dynamics, this quality is not well represented by measures of male body mass.

Data Accessibility

The long-term data used in this study was archived at doi:10.5061/dryad.8vb83 and was also made publicly available by L.L. Getz at: <http://www.life.illinois.edu/getz/>

Acknowledgements

The study was supported by grants SNF #31003A_146445 and ERC #337785 to AO, and by the University of Illinois School of Life Sciences and Graduate College Research Board. We thank the following for their assistance with the field work: D. Tazik, B. McGuire, J. Hofmann, P. Mankin, T. Pizzuto, M. Snarski, S. Buck, K. Gubista, S. Vanthernout, W. Holmgren, P. Malmborg, B. Klatt, L. Gavish, and B. Frase. M. Snarski. We also thank L.-M. Chevin, N. Yoccoz, and three anonymous reviewers for helpful comments on the manuscript.

Author Contribution statement

KB, HF, AO conceived the ideas, designed the methodology, and analysed the data; LG collected the long-term data; HF and KB led the writing of the manuscript; all authors contributed substantially to the manuscript and gave final approval for publication.

References

- Ai, C. & Norton, E.C. (2003) Interaction terms in logit and probit models. *Economics Letters*, 80, 123-129.
- Andreassen, H. P., Glorvigen, P., Rémy, A. & Ims, R. A. (2013) New views on how population-intrinsic and community-extrinsic processes interact during the vole population cycles. *Oikos*, 122, 507-515.
- Batzli, G. O. (1996) Population cycles revisited. *Trends in Ecology & Evolution*, 11, 488-489.
- Boonstra, R., & Boag, P. T. (1987). A Test of the Chitty hypothesis: Inheritance of life-history traits in meadow voles *Microtus pennsylvanicus*. *Evolution*, 41, 929-947.
- Boonstra, R. & Krebs, C. J. (1979) Viability of large- and small-sized adults in fluctuating vole populations. *Ecology*, 60, 567-573.
- Bruna, E.M., Izzo, T.J., Inouyes, B.D. & Vasconcelos, H.L. (2014) Effect of mutualist partner identity on plant demography. *Ecology*, 2014, 95, 3237-3243.
- Burnham, K. P. & Anderson, D. R. (2002) *Model selection and multimodel inference: a practical information-theoretic approach*, Springer Science & Business Media.
- Burthe, S.J., Lambin, X., Telfer, S., Douglas, A., Beldomenico, P., Smith, A. & Begon, M. (2010) Individual growth rates in natural field vole, *Microtus agrestis*, populations exhibiting cyclic population dynamics, *Oecologia*, 162, 653-661.

524 Buston, P. (2003) Social hierarchies: Size and growth modification in clownfish. *Nature*, 424,
525 145-146.

526 Calder, W. A. I. (1984) *Size, Function and Life History*, Cambridge, MA, USA , Harvard
527 University Press.

528 Caswell, H. (2001) *Matrix population models: construction, analysis and interpretation*,
529 second edition, Sunderland, MA, USA, Sinauer.

530 Chitty, D. (1952) Mortality among voles (*Microtus agrestis*) at Lake Vyrnwy,
531 Montgomeryshire in 1936-9. *Philosophical Transactions of the Royal Society of*
532 *London Series B*, 236, 505-552.

533 Christian, J.J. (1950). The adreno-pituitary system and population cycles in mammals.
534 *Journal of Mammalogy*, 247-259.

535 Christian, J.J. & Davis, D.E. (1966) Adrenal glands in female voles (*Microtus*
536 *pennsylvanicus*) as Related to Reproduction and Population Size. *Journal of*
537 *Mammalogy*, 1-18.

538 Coulson, T., Kendall. B., Bartold, J., Plard, F., Schindler, S., Ozgul, A., Gaillard J-M (in
539 review) A framework to model evolutionary and plastic responses of populations to
540 environmental change.

541 Coulson, T. (2012) Integral projections models, their construction and use in posing
542 hypotheses in ecology. *Oikos*, 121, 1337-1350.

543 Coulson, T., Macnulty, D. R., Stahler, D.R., Wayne, R.K. & Smith, D.W. (2011) Modeling
544 effects of environmental change on wolf population dynamics, trait evolution, and life
545 history. *Science*, 334, 1275-1278

546 De Kroon, H., Van Groenendael, J. & Ehrlén, J. (2000) Elasticities: a review of methods and
547 model limitations. *Ecology*, 81, 607-618.

548 De Roos, A., Persson, L. & McCauley, E. (2003) The influence of size-dependent life-history
549 traits on the structure and dynamics of populations and communities. *Ecology Letters*,
550 6, 473-487.

551 Easterling, M. R., Ellner, S. P. & Dixon, P. M. (2000) Size-specific sensitivity: applying a
552 new structured population model. *Ecology*, 81, 694-708.

553 Ellner, Stephen P. & Rees, M. (2006) Integral projection models for species with complex
554 demography. *The American Naturalist*, 167, 410-428.

555 Elton, C. (1924) Periodic fluctuations in number of animals: their causes and effects. *British*
556 *Journal of Experimental Biology*, 2, 119-163.

557 Getz, L. L., Hofmann, J. E., McGuire, B. & Dolan III, T. W. (2001) Twenty-five years of
 558 population fluctuations of *Microtus ochrogaster* and *M. Pennsylvanicus* in three
 559 habitats in east-central Illinois. *Journal of Mammalogy*, 82, 22-34.

560 Getz, L. L., Oli, M. K., Hoffman, J. E. & McGuire, B. (2006) Vole population fluctuations:
 561 factors that initiate and determine intervals between them in *Microtus ochrogaster*.
 562 *Journal of Mammalogy* 87, 387–393.

563 Getz, L. L., Oli, M. K., Hofmann, J. E. & McGuire, B. (2005) Habitat-specific demography of
 564 sympatric vole populations over 25 years. *Journal of Mammalogy*, 86, 561-568.

565 Goswami, V. R., Getz, L. L., Hostetler, J. A., Ozgul, A. & Oli, M. K. (2011) Synergistic
 566 influences of phase, density, and climatic variation on the dynamics of fluctuating
 567 populations. *Ecology*, 92, 1680-1690.

568 Grimm, V. & Uchmański, J. (2002) Individual variability and population regulation: a model
 569 of the significance of within-generation density dependence. *Oecologia*, 131, 196-
 570 202.

571 Hanski, I., Hansson, L. & Henttonen, H. (1991) Specialist predators, generalist predators, and
 572 the microtine rodent cycle. *Journal of Animal Ecology*, 60, 353-367.

573 Kingsolver, J. G. & Pfenning, D. W. (2004). Individual-level selection as a cause of Cope's
 574 rule of phyletic size increase. *Evolution*, 58, 1608-1612.

575 Krebs, C. J. (1996) Population cycles revisited. *Journal of Mammalogy*, 77, 8-24.

576 Krebs, C.J. (2013) Population fluctuations in rodents. University of Chicago Press, 2013.

577 Krebs, C. J. & Myers, J. H. (1974). Population cycles in small mammals. *In*: Macfadyen, A.
 578 (ed.) *Advances in Ecological Research*. Academic Press.

579 Laake, J. & Rexstad, E. (2010) RMark—an alternative approach to building linear models in
 580 MARK. Appendix C in Program MARK: “A Gentle Introduction”. [Online.]
 581 Available at www.phidot.org/software/mark/docs/book.

582 Lidicker, W.Z. (1988) Solving the enigma of microtine “cycles”. *Journal of mammalogy*, 69,
 583 225-235.

584 Lidicker, W.Z. (1991) In defense of a multifactor perspective in population ecology. *Journal*
 585 *of Mammalogy*, 72, 631-635.

586 Lidicker, W. Z. & Ostfeld, R. S. (1991) Extra-large body size in California voles: causes and
 587 fitness consequences. *Oikos*, 61, 108-121.

588 Lima, M., Stenseth, N. C., Yoccoz, N. G. & Jaksic, F. M. (2001) Demography and population
 589 dynamics of the mouse opossum (*Thylamys elegans*) in semi-arid Chile: seasonality,

feedback structure and climate. *Proceedings of the Royal Society of London. Series B: Biological Sciences*, 268, 2053-2064.

Linzey, A. V. & Hammerson, G. (2008) *Microtus ochrogaster* [Online]. Available: www.iucnredlist.org [Accessed 10.08.2010].

Merow, C., Dahlgren, J. P., Metcalf, C. J. E., Childs, D. Z., Evans, M. E. K., Jongejans, E., Record, S., Rees, M., Salguero-Gómez, R. & McMahon, S. M. (2014). Advancing population ecology with integral projection models: a practical guide. *Methods in Ecology and Evolution*, 5, 99-110.

Morhac, M. (2012) Peaks: Peaks. R package version 0.2.

Norrdahl, K., & Korpimäki, E. (2002) Changes in individual quality during a 3-year population cycle of voles. *Oecologia*, 130, 239-249.

O'Riain, M. J. & Jarvis, J. U. M. (1998) The dynamics of growth in naked mole-rats: the effects of litter order and changes in social structure. *Journal of Zoology*, 246, 49-60.

Oli, M. K. (1999) The Chitty effect: a consequence of dynamic energy allocation in a fluctuating environment. *Theoretical Population Biology*, 56, 293-300.

Oli, M. K. & Dobson, F. S. (1999). Population cycles in small mammals: the role of age at sexual maturity. *Oikos*, 86, 557-565.

Oli, M. K., & Dobson, F. S. (2001). Population cycles in small mammals: The α -hypothesis. *Journal of Mammalogy*, 82, 573-581.

Ozgul, A., Getz, L. L. & Oli, M. K. (2004) Demography of fluctuating populations: temporal and phase-related changes in vital rates of *Microtus ochrogaster*. *Journal of Animal Ecology*, 73, 201-215.

Ozgul, A., Childs, D. Z., Oli, M. K., Armitage, K. B., Blumstein, D. T., Olson, L. E., Tuljapurkar, S. & Coulson, T. (2010) Coupled dynamics of body mass and population growth in response to environmental change. *Nature*, 466, 482-485.

Ozgul, A., Bateman, A. W., English, S., Coulson, T. & Clutton-Brock, T. H. (2014) Linking body mass and group dynamics in an obligate cooperative breeder. *Journal of Animal Ecology*, 83, 1357-1366.

Pelletier, F., Clutton-Brock, T., Pemberton, J., Tuljapurkar, S. & Coulson, T. (2007) The evolutionary demography of ecological change: linking trait variation and population growth. *Science*, 315, 1571-1574.

Peters, R. H. (1983) *The ecological implications of body size*, Cambridge, MA, Cambridge University Press.

- R Core Team (2015) R: A language and environment for statistical computing. Vienna, Austria: R Foundation for Statistical Computing.
- Radchuk, V., Ims, R. A., & Andreassen, H. P. (2016). From individuals to population cycles: the role of extrinsic and intrinsic factors in rodent populations. *Ecology*, 97(3), 720-732.
- Stalling, D. T. (1990) *Microtus ochrogaster*. *Mammalian Species*, 355, 1-9.
- Stenseth, N. (1999) Population cycles in voles and lemmings: density dependence and phase dependence in a stochastic world *Oikos*, 87, 427-461.
- Stenseth, N. C., Bjornstad, O. N. & Falck, W. (1996) Is spacing behaviour coupled with predation causing the microtine density cycle? A synthesis of current process-oriented and pattern-oriented studies. *Proceedings of the Royal Society of London B: Biological Sciences*, 263, 1423-1435.
- Sundell, J. & Norrdahl, K. (2002) Body size-dependent refuges in voles: An alternative explanation of the Chitty effect. *Annales Zoologici Fennici* 39, 325-333.
- Turchin, P. & Batzli, G. O. (2001) Availability of food and the population dynamics of arvicoline rodents. *Ecology*, 82, 1521-1534.
- Uchmanski, J. (1985) Differentiation and frequency distributions of body weights in plants and animals. *Philosophical Transactions of the Royal Society B: Biological Sciences*, 310, 1-75.
- White, G. C. & Burnham, K. P. (1999) Program MARK: survival estimation from populations of marked animals. *Bird Study*, 46, 120-139.
- Wood, S. (2006) *Generalized additive models: an introduction with R*, CRC press.

Supporting Information

- The following Supporting Information is available for this article online
- Appendix S1 Sex-specific abundance and average body mass
- Appendix S2 Effect of seasonality
- Appendix S3 Estimation of reproduction probability
- Appendix S4 Retrospective perturbation analysis
- Appendix S5 Single-time-step transient analysis

Table 1. Models indicating the relationships between body mass, phase and the demographic and trait-transition rates. The most parsimonious model, determined by AICc model selection, is shown in bold for each trait (see methods). The effect of dropping a term from or adding a term to the model on the AICc score is shown; positive ΔAICc values indicate that the altered model had less support compared to the most parsimonious model. $s(\text{mass})$ indicates a non-linear, spline term.

Response	n	Random effects	Fixed effects	ΔAICc
Survival	6484		mass + mass² + stage + phase + stage x phase + mass x phase + mass² x stage	0
			– mass ² x stage	2.52
			– mass x phase	10.15
			– stage x phase	10.28
			– stage - stage x phase - mass ² x stage	28.45
			– mass ² - mass ² x stage	36.73
			– mass - mass ² - mass x phase - mass ² x stage	93.14
			– phase - stage x phase - mass x phase	190.79
Recapture	6484		stage + phase + stage x phase	0
			– stage x phase	16.30
			– phase - stage x phase	24.97
			– stage - stage x phase	79.57
Maturation	6484		mass + mass² + phase	0
			+ phase x mass	6.01
			– mass ²	2.10
			– mass - mass ²	8.74
			– phase	45.22
Reproduction	4816	month	mass + phase	0
			– mass	28.75
			– phase	9.55
Growth	2719	month + id	s(mass) + phase + s(mass) x phase	0
			+ stage	1.93
			– s(mass) x phase	12.98
			– s(mass) - s(mass) x phase	1510.4
			– phase - s(mass) x phase	75.90
Offspring mass	189		phase	0
			+ mass	2.10
			+ mass + mass x phase	8.27
			- phase	14.03

Figures

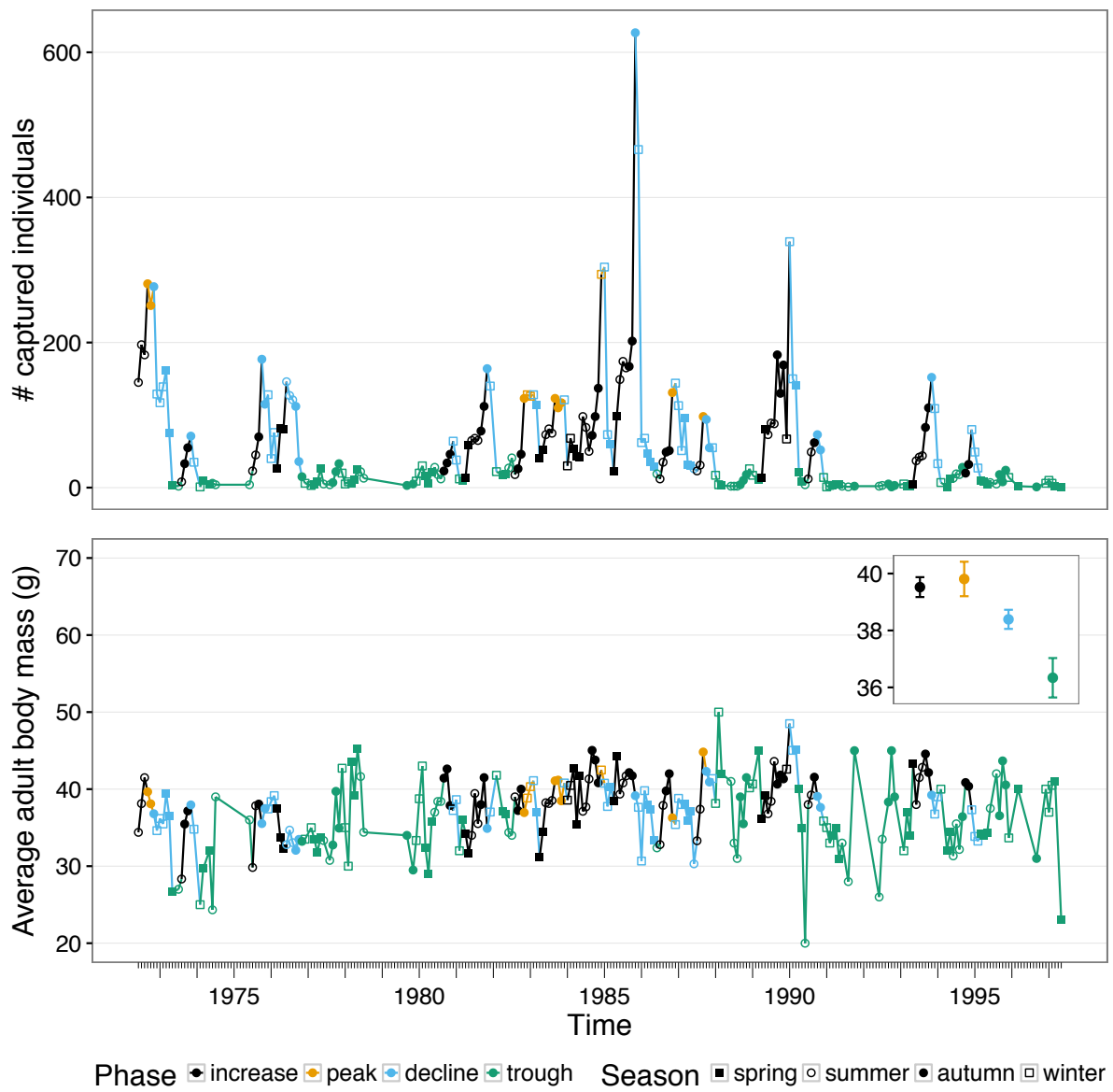
Figure 1. a) Total number of captured individuals during monthly captures. b) Fluctuations of average male adult body mass over the study period. The inset shows the mean body mass of all individuals per phase with 95% confidence intervals. Colours indicate the assigned phases, while the shape of the points indicate the season.

Figure 2. Schematic representation of the perturbation analyses. 1) The IPMs we developed consisted of 7 underlying functions: juvenile survival (S_j), adult survival (S_a), maturation rate (M), probability of being reproductive (R), per capita fecundity (F), ontogenetic growth (G) and inheritance (D). Together these functions can project a population distribution from time t to time $t+1$. Furthermore they are characterized by an asymptotic growth rate (λ). 2) Mixed IPMs were generated, where each of the underlying functions was parameterized in either of two distinct phases. We tested all combinations, leading to a total of $2^7 = 128$ IPMs. For each mixed IPM the asymptotic growth rate was estimated. 3) We regress these 128 values of λ on the structure of the IPM that they were generated from. This structure is characterized by seven dummy variables (P), each of which represents one of the seven underlying function. Depending on whether the function it represents was parameterized in phase 1 or in phase 2, the variable had the value 0 or 1 respectively. The regression coefficients (β 's) of this regression, represent the importance of each of the seven functions in shaping population and trait dynamics.

Figure 3. Estimated trait-demography relationships. Shaded areas indicate 95% confidence intervals. a) Juvenile survival, b) adult survival, c) maturation rate, and d) reproduction probability, and e) body mass at next time step as a function of the current body mass.

Figure 4. Retrospective perturbation analysis of the changes in predicted (a-c) population growth rate and (d-f) adult body mass during three phase transitions. The asymptotic results are shown in black, the transient (four time-step) results in grey. Each bar indicates the contribution of a life-history component on the predicted change. The life-history processes are S_j : juvenile survival, S_a : adult survival, G : growth, M : maturation, R : reproduction probability, F : fecundity, and D : inheritance (i.e., offspring trait value).

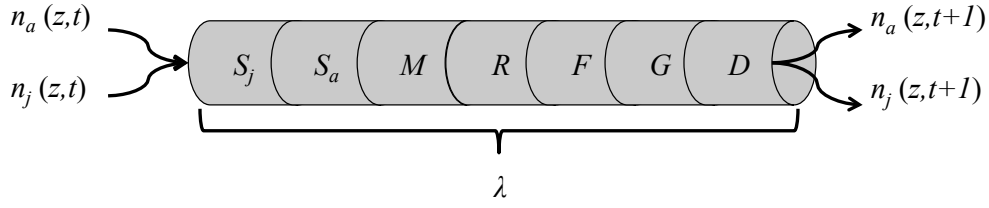
690



691

692 Figure 1

1. General IPM



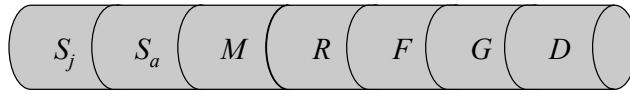
2. Composite IPMs



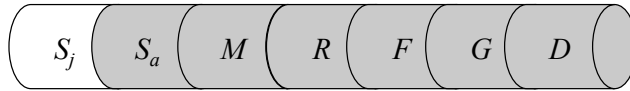
Phase 1



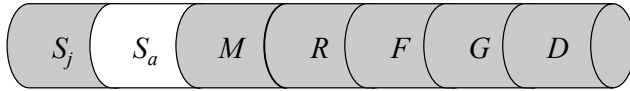
Phase 2



λ_1



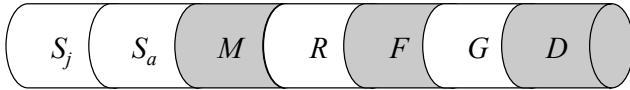
λ_2



λ_3

:

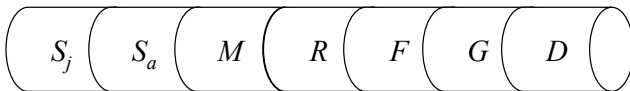
:



λ_{44}

:

:



$\lambda_{128} (=2^7)$

3. Contributions (β)



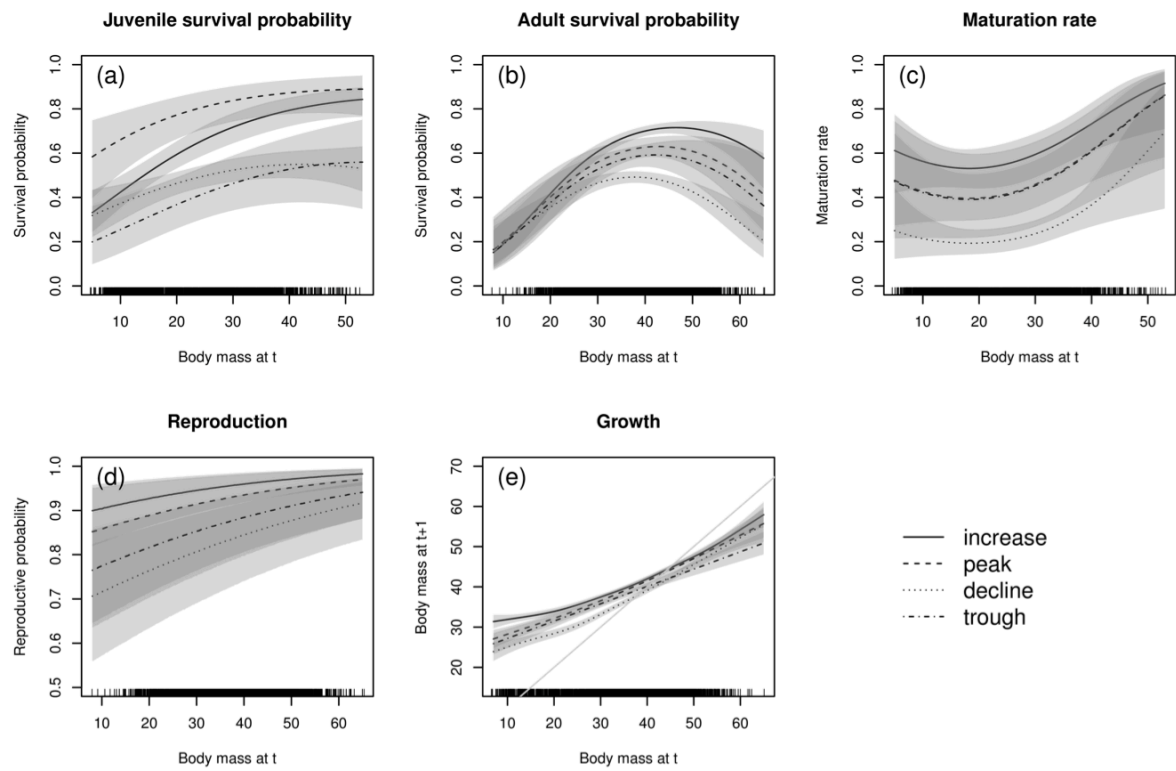
$\rightarrow p_j = 0$



$\rightarrow p_j = 1$

$$\lambda_i = \mu + \beta_{S_j} p_{S_j, i} + \beta_{S_a} p_{S_a, i} + \beta_M p_{M, i} + \beta_R p_{R, i} + \beta_F p_{F, i} + \beta_G p_{G, i} + \beta_D p_{D, i} + \varepsilon_i$$

695



696

697 Figure 3

698

699

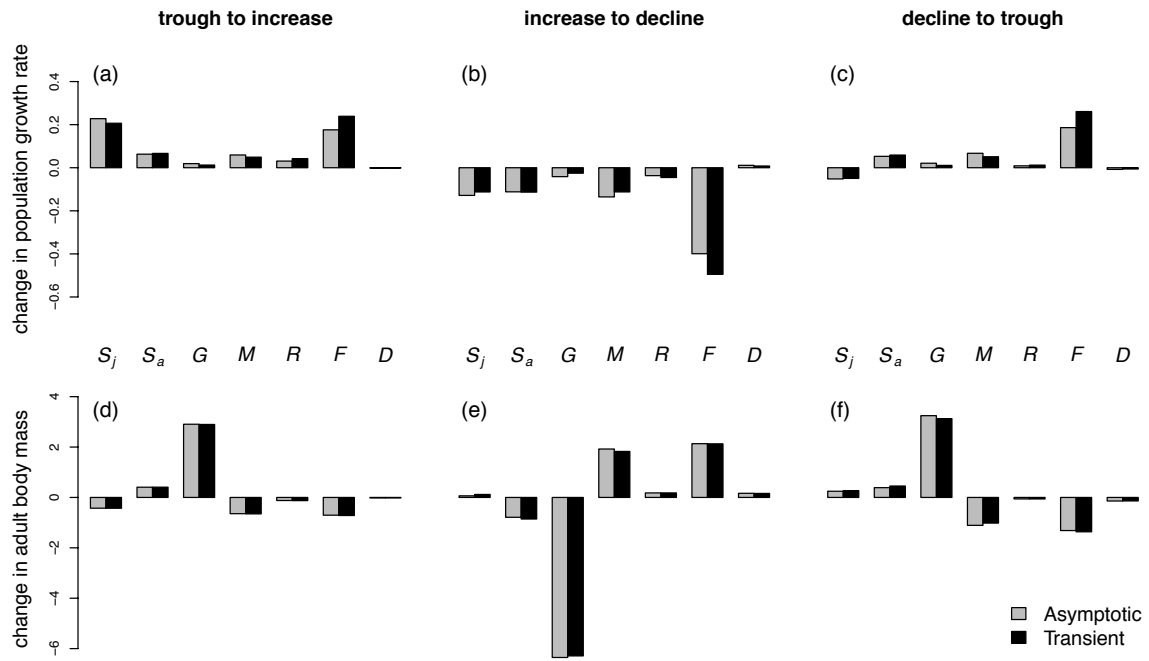


Figure 4